Supporting Information

Defect-Engineered Room Temperature Negative Differential Resistance in Monolayer MoS_2 Transistors

1. The Raman spectra of the monolayer MoS_2 treated with KOH for different soaking durations.

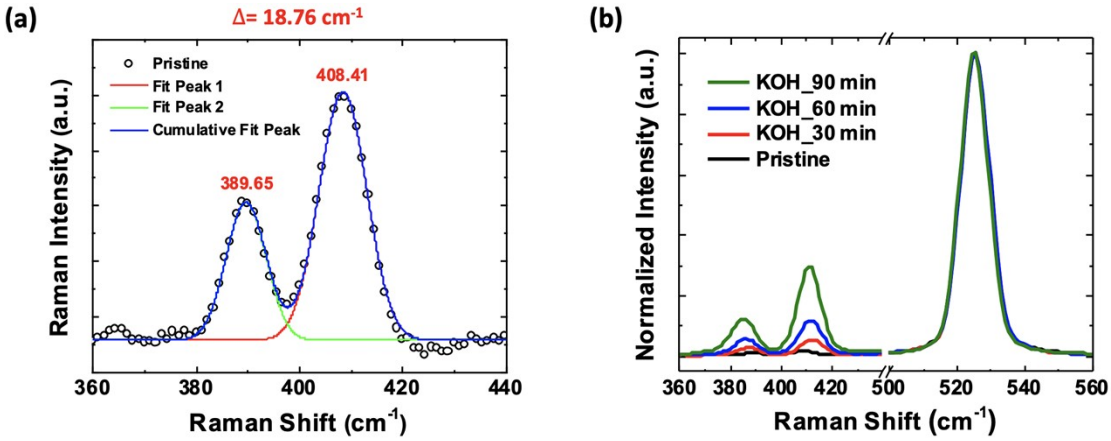

Figure S1. (a) The Raman spectroscopy of pristine monolayer MoS_2 with fitting curves. The separation between E_{2g} (~ 389.65 cm^{-1}) and A_{1g} (~ 408.41 cm^{-1}) is ~ 18.76 cm^{-1} indicating monolayer MoS_2 at room temperature. **(b)** Comparison of Raman spectra for different monolayer MoS_2 samples treated with KOH in 0, 30, 60 and 90-minute durations, respectively, in which all curves are normalized to the intensity of silicon peak. It turns out that the Raman peak position of silicon for all conditions are the same, indicating that the E_{2g} and A_{1g} Raman shifts of KOH-treated monolayer MoS_2 are not affected by our measurement setup.

2. Preliminary experiments of e-beam bombarded monolayer MoS_2 for different conditions of acceleration voltage and beam current.

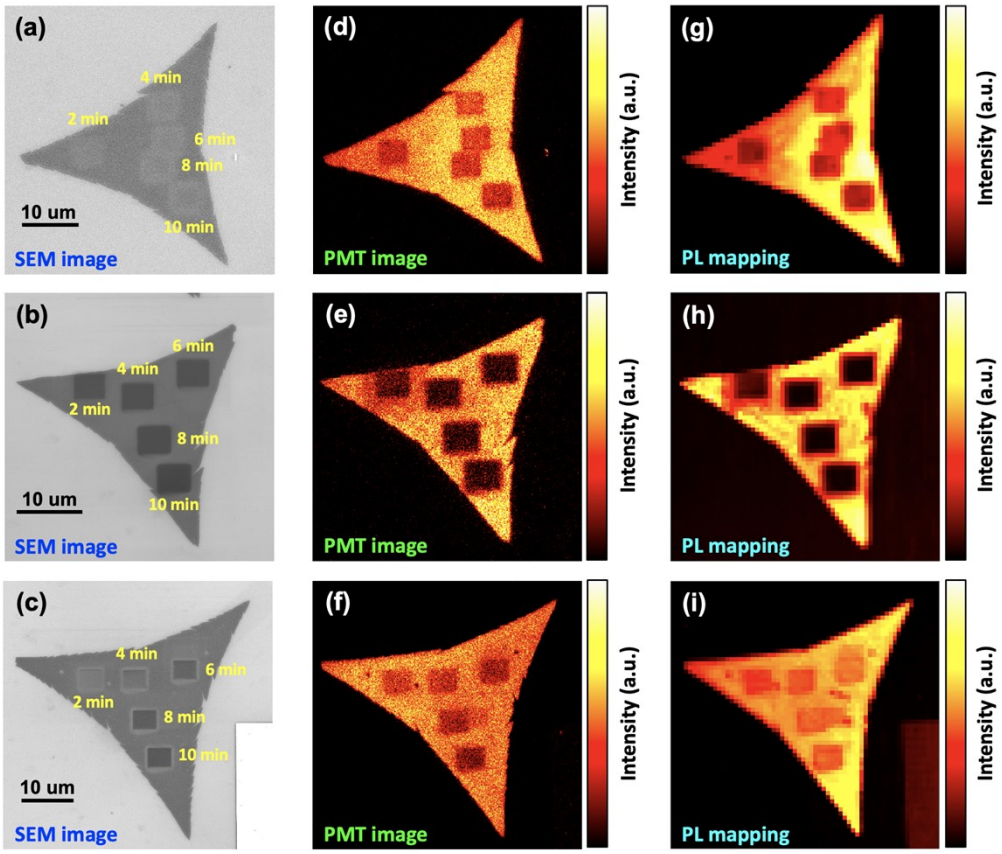

Figure S2. Several preliminary experiments with different acceleration voltages (V_{acc}) and beam currents (I) are conducted in order to adopt a proper condition to create S-vacancy in monolayer MoS_2. **(a-c)** The SEM images of three samples bombarded under three conditions: **(a)** $V_{acc} = 15\ kV$ and $I = 0.49\ nA$; **(b)** $V_{acc} = 10\ kV$ and $I = 0.49\ nA$; **(c)** $V_{acc} = 10\ kV$ and $I = 1.49\ nA$, respectively. Five rectangular areas of $\sim 4 \times 5\ \mu m^2$ with different exposure times are bombarded in each monolayer MoS_2. The corresponding PMT and PL mapping images are shown in **(d-f)** and **(g-i)**, respectively. Consequently, the appropriate condition for creating S-vacancy without damaging the material severely is using $V_{acc} = 15\ kV$ and $I = 0.49\ nA$.

3. The e-beam bombarded monolayer MoS_2 with different dosages.

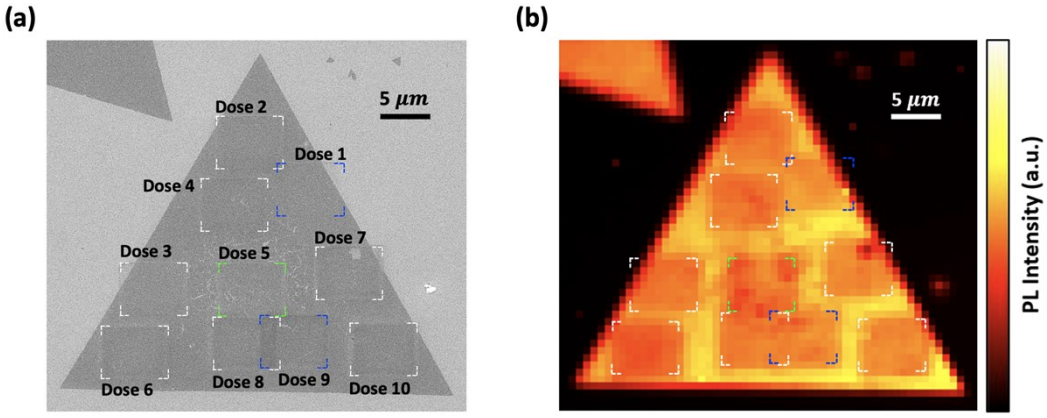

Figure S3. (a-b) The SEM image and its corresponding PL mapping image of the monolayer MoS_2 on gold substrate. The e-beam bombardment conditions are $V_{acc} = 15\ kV$ and $I = 0.49\ nA$ with different dosages from $\sim 0.83 \times 10^5\ \mu C\ cm^{-2}$ (Dose 1) to $\sim 8.28 \times 10^5\ \mu C\ cm^{-2}$ (Dose 10), which can be calculated by the formula of $Dose = I \times t/A(C\ cm^{-2})$.

4. XPS analysis of e-beam bombarded monolayer MoS_2 with different dosages.

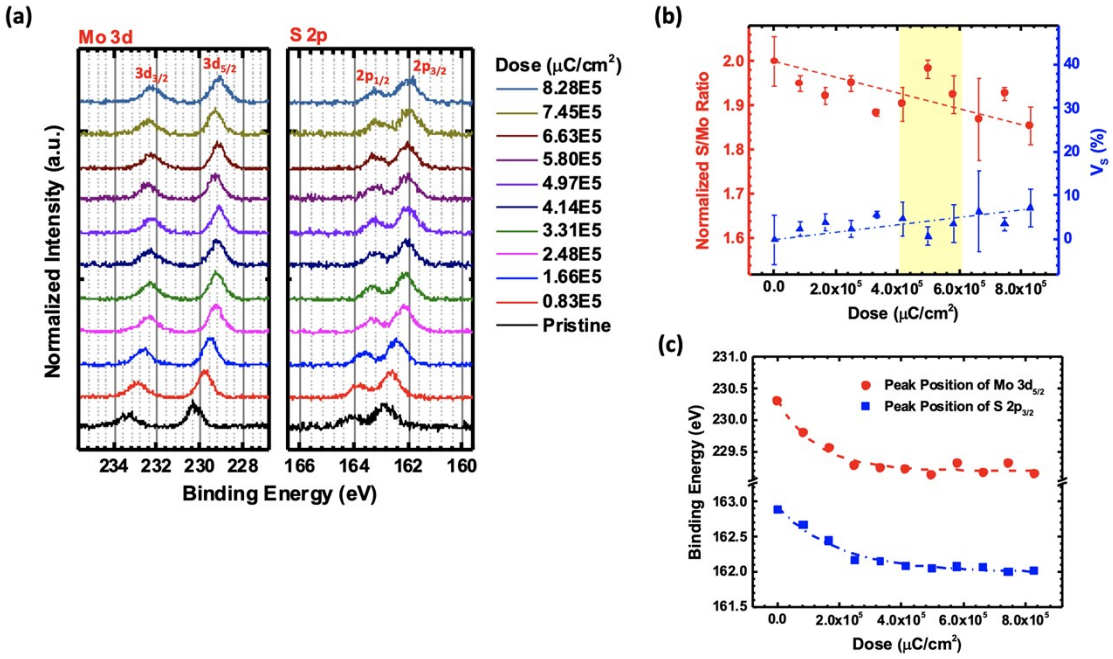

Figure S4. (a) XPS of Mo 3d (left panel) and S 2p (right panel) for various e-beam dosages. The material is transferred on gold substrate in order to minimize the charging effect during the XPS experiment, and all data have been calibrated to the binding energy of Au (84 eV). **(b)** Normalized S/Mo ratio (left y-axis) and the percentage of S-vacancy (V_S) (right y-axis) as a function of dosage showing a decreasing S/Mo ratio and an increasing S-vacancy with increasing dosage. The S-vacancy of $\sim 4.5 \pm 1\ \%$ can be created with the dosage from $\sim 4 \times 10^5$ to $6 \times 10^5\ \mu C\ cm^{-2}$ as demonstrated within the yellow region. **(c)** Both peak position of S $2p_{3/2}$ and Mo $3d_{5/2}$ shift to lower binding energy with increasing dosage indicating that more S-vacancy are formed in the MoS_2 resulting in a metallic-like behavior.

5. Electrical characteristics of the other monolayer MoS_2 FET treated with KOH for 30 minutes.

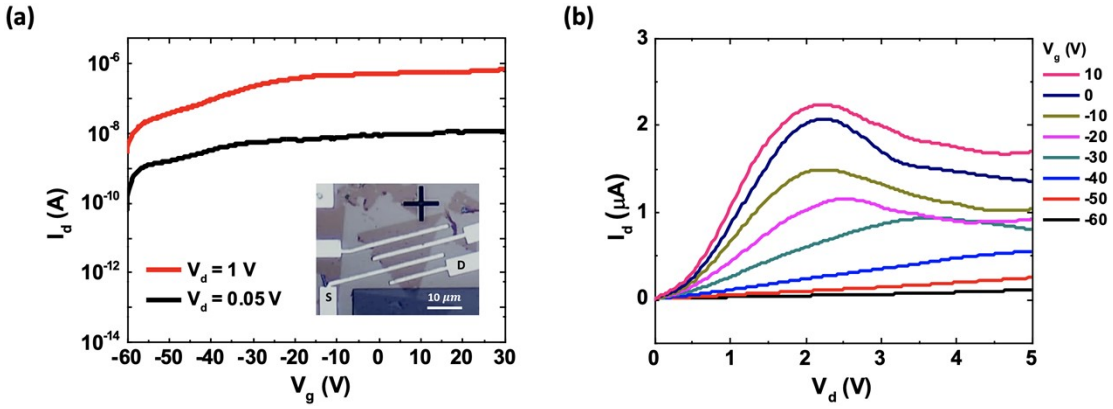

Figure S5. (a) I_d-V_g characteristics of the monolayer MoS_2 FET treated with KOH for 30 minutes showing a metallic-like behavior. The OM image of the measured device is presented in the inset. **(b)** The NDR behavior can be observed in the I_d-V_d curves.

6. Electrical characteristics of e-beam bombarded monolayer MoS_2 FET.

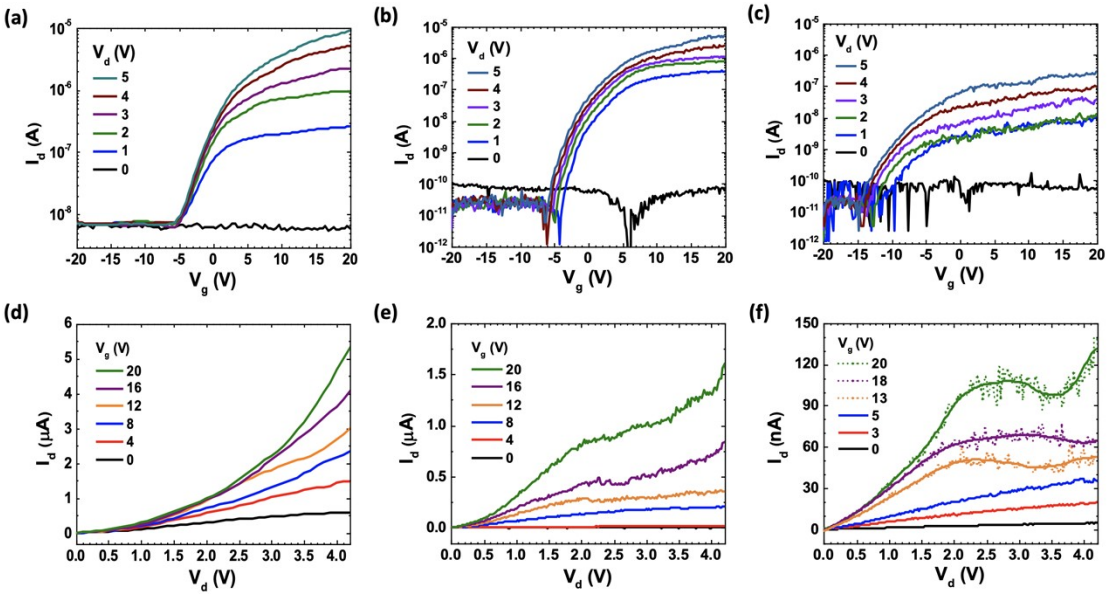

Figure S6. I_d-V_g characteristics of the monolayer MoS_2 FET at varying bias voltages for **(a)** pristine and **(b-c)** e-beam bombarded with the dosage of $\sim 2.5 \times 10^5$ and $\sim 5 \times 10^5\ \mu C\ cm^{-2}$, respectively. The acceleration voltage and beam current are $V_{acc} = 15\ kV$ and $I = 0.49\ nA$, respectively. **(d-f)** The I_d-V_d characteristics at varying gate voltages corresponding to the dosage conditions of (a-c). **(f)** The NDR behavior can be observed under a dosage of $\sim 5 \times 10^5\ \mu C\ cm^{-2}$ corresponding to $V_S \sim 5\ \%$. Dots and solid lines shown in the I_d-V_d curves at $V_g = 13, 18, 20\ V$ indicate raw data and guide to the eyes, respectively.

7. XPS of the as-grown monolayer MoS_2 flakes with different amount of S-vacancy.

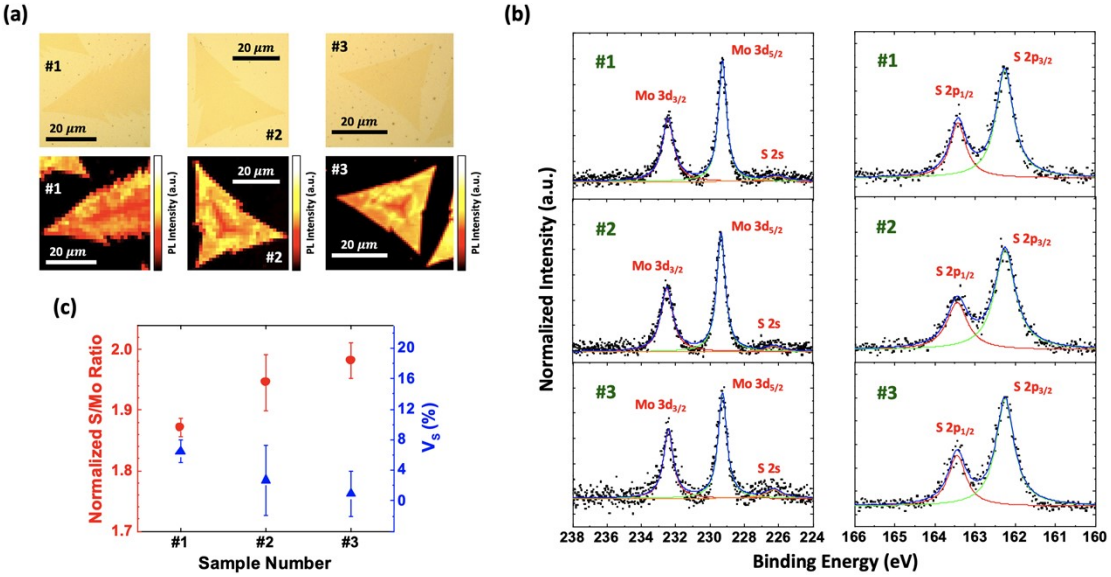

Figure S7. XPS analysis of as-grown MoS_2 with different amount of S-vacancy. **(a)** OM (top panel) and PL mapping (bottom panel) images of the as-grown MoS_2 samples. It turns out that different profiles of the monolayer MoS_2 correspond to different amount of S-vacancy. **(b)** Mo 3d and S 2p spectroscopy of the as-grown MoS_2 for three kinds of samples indicated as #1 to #3 in **(a)**. **(c)** The normalized S/Mo ratio (left axis) and the percentage of S-vacancy (right axis) for three different samples.

8. XPS analysis of the as-grown monolayer MoS_2 FET with $V_S \sim 5\,\%$.

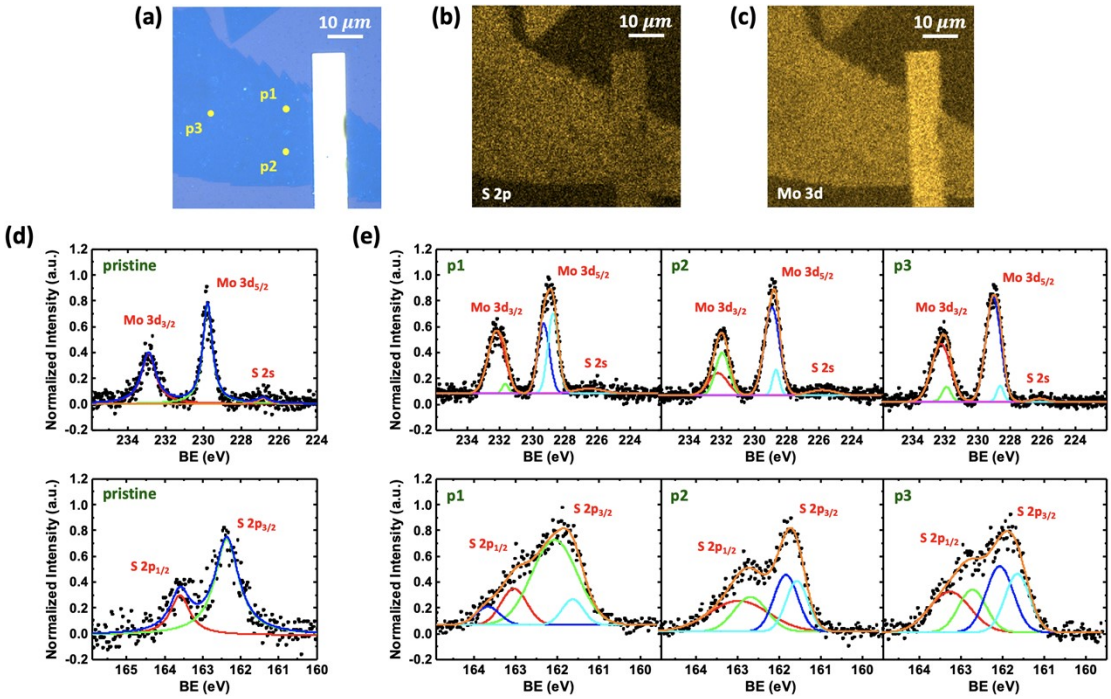

Figure S8. (a) OM image of the as-grown monolayer MoS_2 FET. **(b-c)** The XPS mapping image of the S 2p and Mo 3d, respectively, showing the uniform quality of the as-grown monolayer MoS_2. **(d)** The XPS spectra of the Mo 3d (top panel) and S 2p (bottom panel) for the pristine monolayer MoS_2 by typical CVD method. **(e)** The XPS spectra of the Mo 3d (top panel) and S 2p (bottom panel) for the measured device shown in (a) which is synthesized by CVD method under the condition of low S supply. Three analyzed points (p1 to p3) are indicated as yellow dots in the OM image of (a). The S-vacancy is determined to $\sim 5\,\%$ from the average value of three measured positions, compared to the XPS data of the pristine MoS_2 as shown in (d).

9. Electrical characteristics of the as-grown monolayer MoS_2 FET with $V_S \sim 5\ \%$.

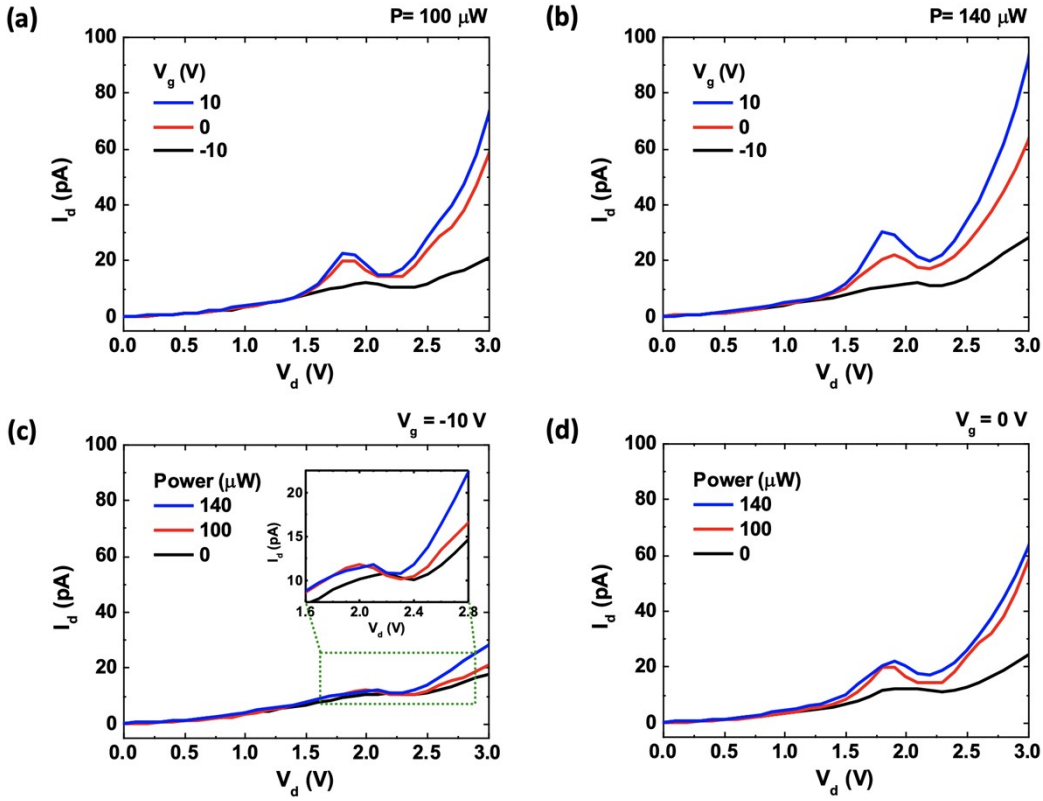

Figure S9. (a-b) The I_d-V_d characteristics of the as-grown MoS_2 FET applied with different gate voltage V_g with a fixed power of light illumination $P = 100, 140\ \mu W$, respectively. A larger peak to valley ratio can also be observed at higher power of light. **(c-d)** The I_d-V_d characteristics of the as-grown MoS_2 FET illuminated with different power of light at a fixed gate voltage $V_g = -10, 0\ V$, respectively. The NDR behavior can be seen clearly in the inset of (c), which is partially enlarged region from its original I_d-V_d curves.

10. Electrical characteristics and XPS of the as-grown monolayer MoS_2 FET with $V_S \sim 4.5\ \%$.

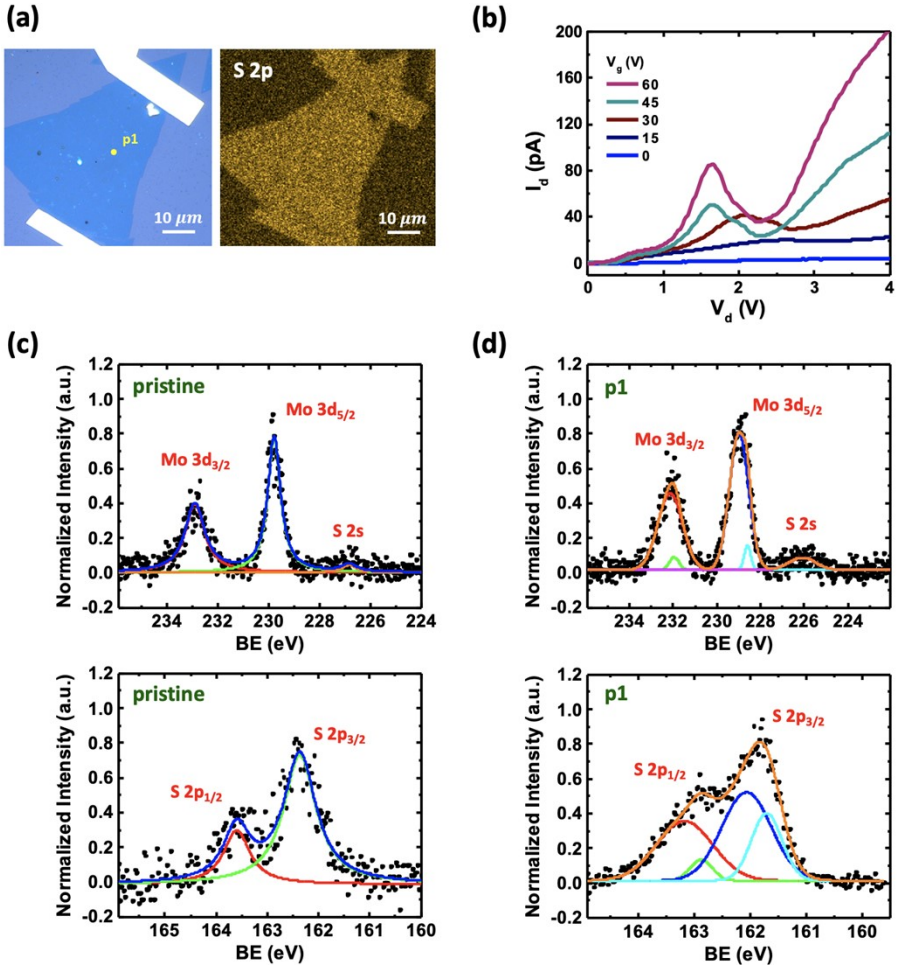

Figure S10. (a) OM image of another as-grown monolayer MoS_2 FET (left panel) and its corresponding XPS S2p mapping image (right panel) showing the uniform quality of the as-grown monolayer MoS_2. **(b)** The I_d-V_d curves clearly demonstrate the NDR behavior. **(c)** The XPS spectra of the Mo 3d (top panel) and S 2p (bottom panel) for the pristine monolayer MoS_2 synthesized by typical CVD method. **(d)** The XPS spectra of the Mo 3d (top panel) and S 2p (bottom panel) for the measured device shown in (a) synthesized by CVD method under the condition of low S supply. The analyzed point (p1) is indicated as yellow dot in the OM image of (a). The S-vacancy is determined to

~ 4.5 %, compared to the XPS data of the pristine MoS_2 as shown in (c).

11. The reproducible NDR behavior in the other as-grown monolayer MoS_2 FET.

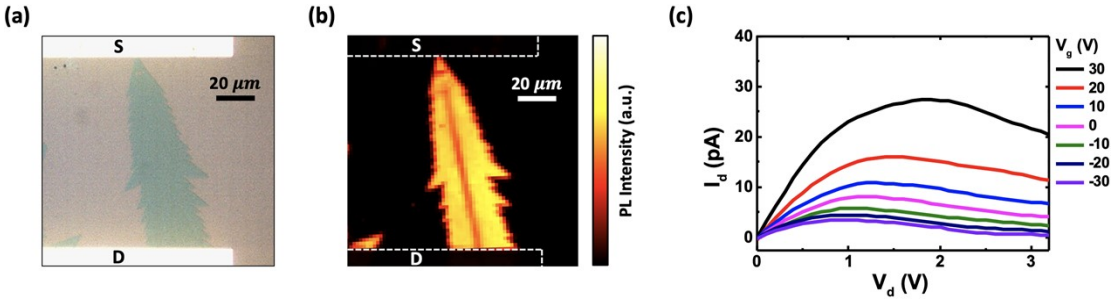

Figure S11. (a-b) The OM image and its corresponding PL mapping image of the other as-grown monolayer MoS_2 FET, respectively. **(b)** The reproducible NDR behavior can be seen in the I_d-V_d curves.

12. Simulation of the band structures for various percentage of S-vacancy.

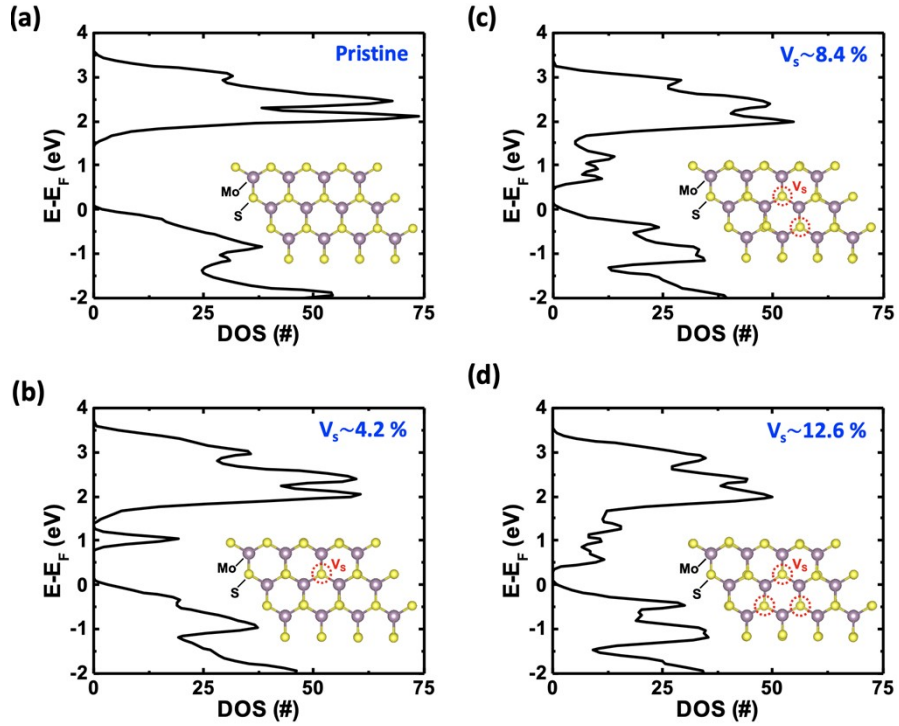

Figure S12. (a-d) The density of state (DOS) for monolayer MoS_2 with different S-vacancy concentrations investigated by density-functional theory (DFT) simulation using the Vienna ab initio simulation package (VASP). The DOS of monolayer MoS_2 with S-vacancy ranging from pristine to 12.6 % is calculated by removing zero to three sulfur atoms in the 3×4×1 supercell. The insets present the schematics of the atomic structure, in which the sulfur, molybdenum atoms and S-vacancy are indicated as yellow sphere, purple sphere and red dotted circle, respectively.